SUPPLEMENT

Deletion of Kir5.1 impairs renal ability to excrete K^+ during increased dietary K^+ intake

Peng Wu*, Zhong-Xiuzi Gao*, Dan-Dan Zhang, Xiao-Tong Su, Wen-Hui Wang and Dao-Hong Lin

Department of Pharmacology, New York Medical College, Valhalla, NY, 10595.

Supplemental Table of Contents

Methods

Preparation of the DCT Mice were sacrificed by cervical dislocation after anesthesia with 2% isoflurane and the abdomen was opened to expose the left kidney. We perfused the left kidney with 2 ml L-15 medium (Life Technology) containing Type 2 collagenase (250 unit/ml) and then removed the collagenase-perfused kidney. The renal cortex was separated and further cut into small pieces for additional incubation in collagenase-containing L-15 media for 30-50 min at 37°C. The tissue was then washed three times with fresh L-15 medium and transferred to an ice-cold chamber for dissection. We identified DCT1 using glomerulus as a mark and the patch-clamp experiments for the

measurement of whole cell K^+ currents were performed in the first 100 μm of the DCT after the glomerulus. We performed the patch-clamp experiments for studying ENaC activity in the last 100 μm DCT before the transition between the DCT and CNT. Since the diameter of the DCT2 is normally larger than the CNT, this anatomic characterization has been used to determine the end of the DCT or the start of the CNT. The isolated DCT tubules were placed on a small cover glass coated with poly-lysine and the cover glass was placed on a chamber mounted on an inverted microscope.

Single channel recording Single channel patch-clamp experiments were performed in the basolateral membrane of both early DCT (DCT1) and late DCT (DCT2). Single K^+ channel currents were recorded with an Axon200B amplifier (Axon), low-pass filtered at 1 KHz, and digitized by an Axon interface (Digidata 1332) with sampling rate of 4 KHz. For the calculation of channel numbers, we selected a channel recording at least 10 min long. We determine the channel open probability (P_o) from the channel number (N) and NP_o (a product of channel number and open probability) which was calculated from data samples of 60 seconds duration in the steady state. NP_o was determined using the following equation:

$$NP_o = \Sigma(t_1 + 2t_2 + ...it_i)$$

where t_i is the fractional open time spent at each of the observed current levels. The channel conductance was determined by measuring the current amplitudes over several voltages.

Whole cell recording Whole-cell patch-clamp experiments were performed in the DCT1. An Axon 200A amplifier was used for the measurement of K^+ reversal potential, Ba^{2+}–sensitive K^+ currents and amiloride-sensitive Na^+ currents. For measuring K^+ reversal potential, the tip of the pipette was filled with pipette solution containing (in mM) 140 KCl, 2 $MgCl_2$, 1 EGTA, 2 MgATP and 5 HEPES (pH 7.4). The pipette was then back-filled with the pipette solution containing amphotericin B (20 μg/0.1 ml). In some experiments, we used low Cl pipette solution containing 125 mM K^+-gluconate, 15 mM KCl, 2 mM MgATP, 1 mM EGTA and 10 mM HEPES (PH=7.4) for the measurement of K^+ reversal potential. Since no significant differences between high and low Cl^- in the pipette were identified, data were pooled. The bath solution is the same as the one we used to perform the single channel recordings. For the measurement of whole-cell Ba^{2+}–sensitive K^+ current, the bath solution contains (in mM) 140 KCl, 2 $MgCl_2$, 1.8 $CaCl_2$ and 10 HEPES (pH=7.4). For measurement of ENaC activity, the tip of the pipette was filled with pipette solution containing 125 mM K+-gluconate, 15 mM KCl, 2 mM MgATP, 1 mM EGTA 10 mM HEPES (PH=7.4). The pipette was then back-filled with amphotericin B (20 μg/0.1 ml) containing the pipette solution. The bath solution contains 130 mM Na^+-gluconate, 10 mM NaCl, 5 mM KCl, 2 mM CaCl2, 2 mM MgCl2 and 10 mM HEPES (pH=7.4) for Na+ currents. After forming a high resistance

seal (>2 GΩ), the membrane capacitance was monitored until the whole-cell patch configuration was formed. The currents were low-pass filtered at 1 KHz, digitized by an Axon interface with 4 KHz sampling rate (Digidata 1440A). Data were analyzed using the pClamp software system 9.0 (Axon).

Immunoblotting Whole kidney protein extract was obtained from frozen kidney homogenized in a buffer containing 250 mM sucrose, 50 mM Tris-HCl pH 7.5, 1 mM EDTA, 1mM EGTA, 1 mM DTT supplemented with phosphatase and protease inhibitor cocktails (Sigma). Protein (40-60 μg) was separated on 4-12% (wt/vol) Tris-Glycine gel (Thermo Fisher Scientific) and transferred to nitrocellulose membrane. The membranes were incubated 1 hour with LI-COR blocking buffer (PBS) and then incubated overnight at 4ºC with anti-NCC (Millipore) and anti-pNCC at threonine-53 antibodies (Phospho Solution) (both 1:6000). An Odyssey infrared imaging system (LI-COR) was used to capture the images at a wave-length of 680 or 800 nM.

Procedures for renal clearance Animal were anesthetized by 2-4% isoflurane through inhaling mask. The mice were placed on a heated small blanket to maintain body temperature at 37ºC. The trachea was cannulated to clear any mucus that may be produced during the experiment. A carotid artery was catheterized with PE10 tubing for blood collection, jugular vein was also cannulated for iv infusion. The bladder was exposed and catheterized via a suprapubic incision with a 10 cm piece of PE-10 tubing for urine collections. After completion of surgery, isotonic saline was given intravenously for 4 hr (0.2-0.3 ml/1 hr and total 0.8-1.2 ml 0.9% saline) to replace surgical fluid losses and to maintain hemodynamics. Urine collections started one hr after infusion of 0.3 ml saline and total 6 collections (every 30 minutes) were performed (2 for controls and 4 for experiments). After renal clearance experiment, the mice were sacrificed by IV somnasol.

RT-PCR of Nedd4-2 The RNA of the isolated DCT and CCD was isolated with RNAqueous-Micro kit (Ambion). The cDNA was generated with Affinity Script RT enzyme from Stratagene (La Jolla, CA). Briefly, 1 μl random primer and 100 ng RNA or single tubule lysate was annealed at 95°C by adding 1 μl DTT, dNTP, and enzyme. The mixture was incubated for 1 hour at 65°C. The Nedd4l primers (2.5 μl, 12.5 nM) were mixed with 2 μl cDNA (200 ng) and 12.5 μl 2× SYBR Green master. MxPro3000 (Stratagene) was used to carry out the experiments, and we used $2^{-\Delta\Delta CT}$ to analyze the comparative expression level of Nedd4l. GAPDH was used as a control. We repeat with primers for Nedd4-2 and Gapdh from OriGene (Rockville, MD). The sequence of Nedd4l is TAGCCTCAGCTCGCCAACAGTA (forward) and GGAGTTGTAAGGTGATGGCTGAG (reversed). The sequence of Gapdh is CATCACTGCCACCCAGAAGACTG (forward); and ATGCCAGTGAGCTTCCCGTTCAG (reversed)

Results

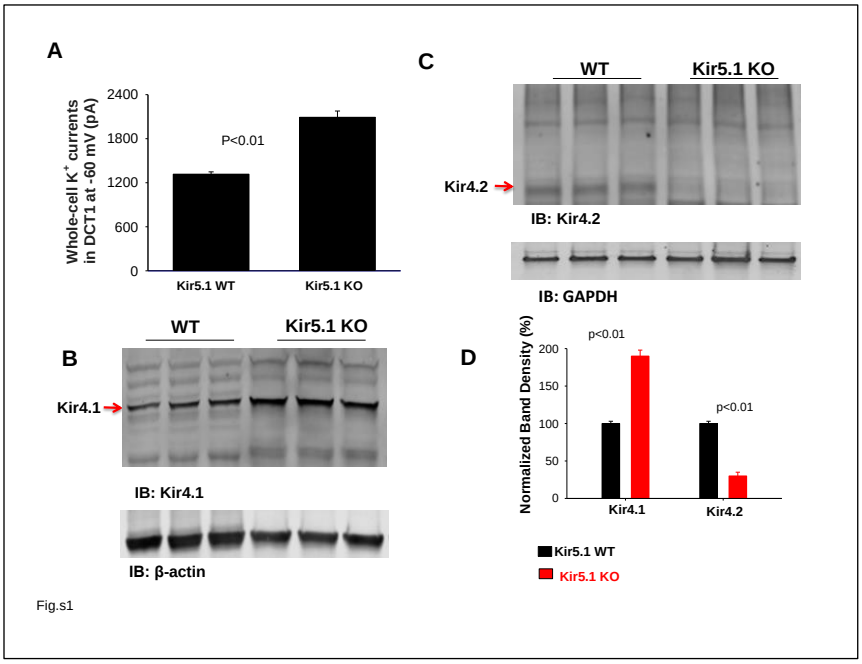

Fig.s1 **Deletion of Kir5.1 increases basolateral K^+ conductance**. (**A**) A bar graph summarizes the values measured at –60 mV with whole-cell recording in the DCT of WT and Kir5.1 KO mice (n=7 or 10). (B) A western blot showing the expression of Kir4.1 in Kir5.1 WT and Kir5.1 KO mice, respectively. A red arrow indicates the Kir4.1 band (The specificity of the antibody was verified using tissue of Kir4.1 KO mice. (C) A western blot showing the expression of Kir4.2 in Kir5.1 WT and Kir5.1 KO mice, respectively. A red arrow indicates the Kir4.2 band (The specificity of the antibody was verified using tissue of Kir4.2 KO mice). (D) Normalized band density of Kir4.1 and Kir4.2 expression in WT and Kir5.1 KO mice.

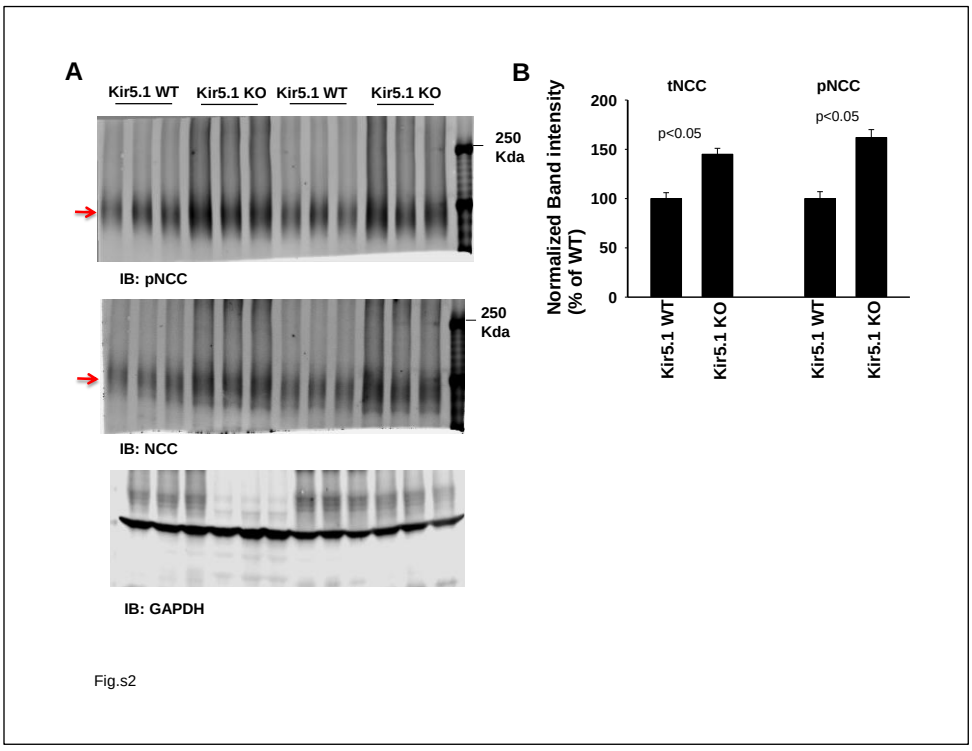

Fig. s2 **Deletion of Kir5.1 increases NCC expression** (A) A immunoblot showing the expression of phosphorylated NCC (pNCC) and total NCC (tNCC) in WT and Kir5.1 KO mice. A red arrow indicates the band for pNCC and NCC. (**B**) A bar graph summarizes the normalized band intensity of the expression of total NCC (NCC) and phosphorylated NCC (pNCC) in WT and Kir5.1 KO mice (n=6). The significance was determined by *t* test.

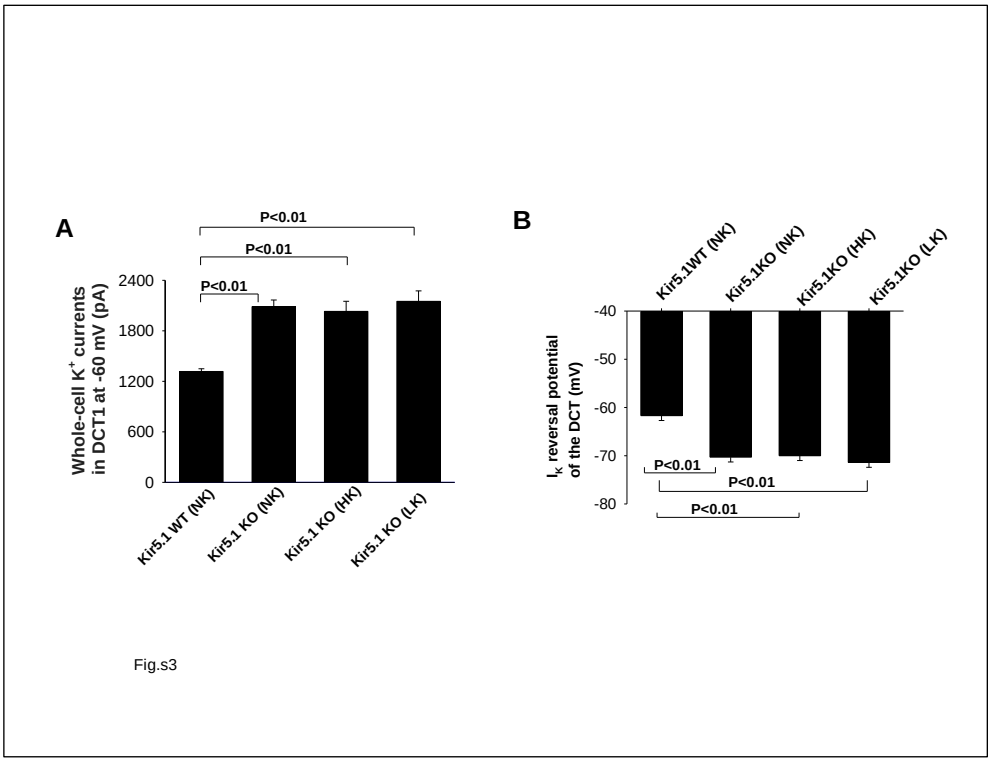

Fig.s3 **Deletion of Kir5.1 eliminates the effect of dietary K^+ intake on the basolateral K^+ conductance in the DCT** (A) A bar graph summarizes the values measured at –60 mV with whole-cell recording (n=6 or 7) in the DCT of WT on NK and Kir5.1 KO mice on NK, HK and LK for 7 days. (**B**) A bar graph summarizes the results of experiments in which I_K reversal potential was measured in WT on NK and Kir5.1 KO mice on NK, HK, and LK diets for 7 days, respectively (n=6). The significance was determined by one way ANOVA.

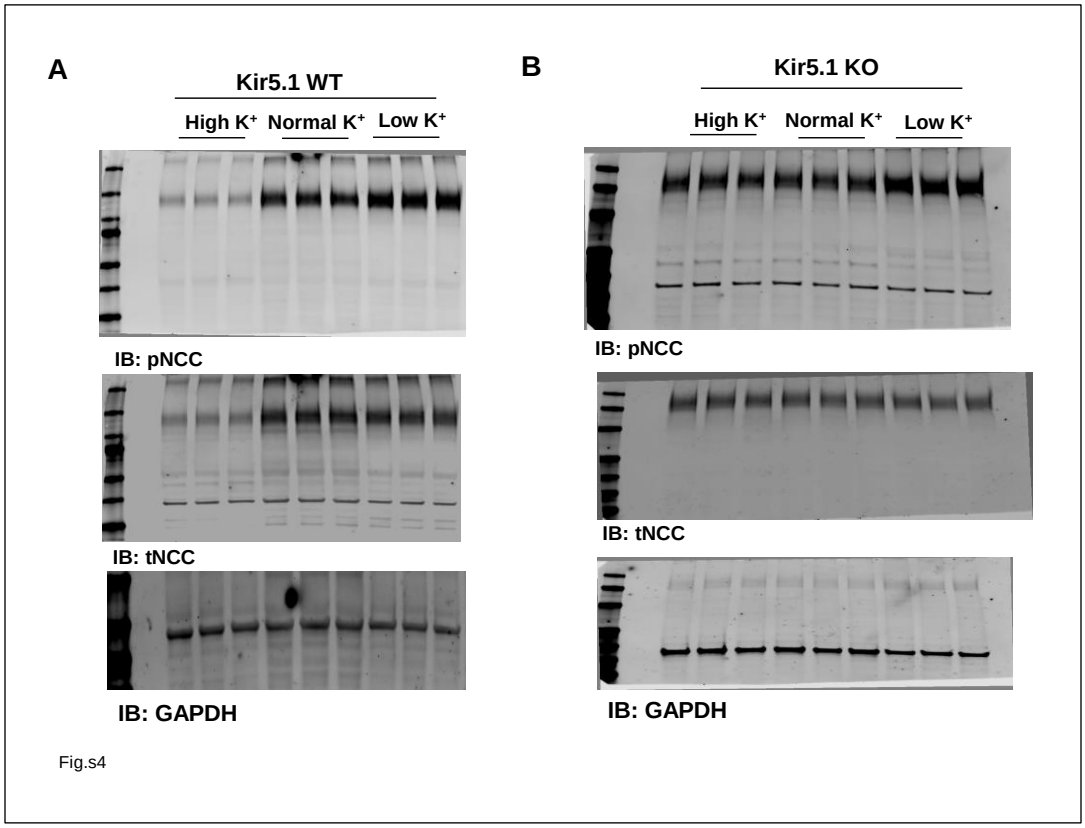

Fig.s4 **Deletion of Kir5.1 abolishes the effect of dietary K^+ intake on tNCC and pNCC**. A full-length immunoblotting showing the expression of pNCC and tNCC in WT (**A**) and in Kir5.1 KO mice. (**B**) on NK, HK, and LK diets for 7 days, respectively.

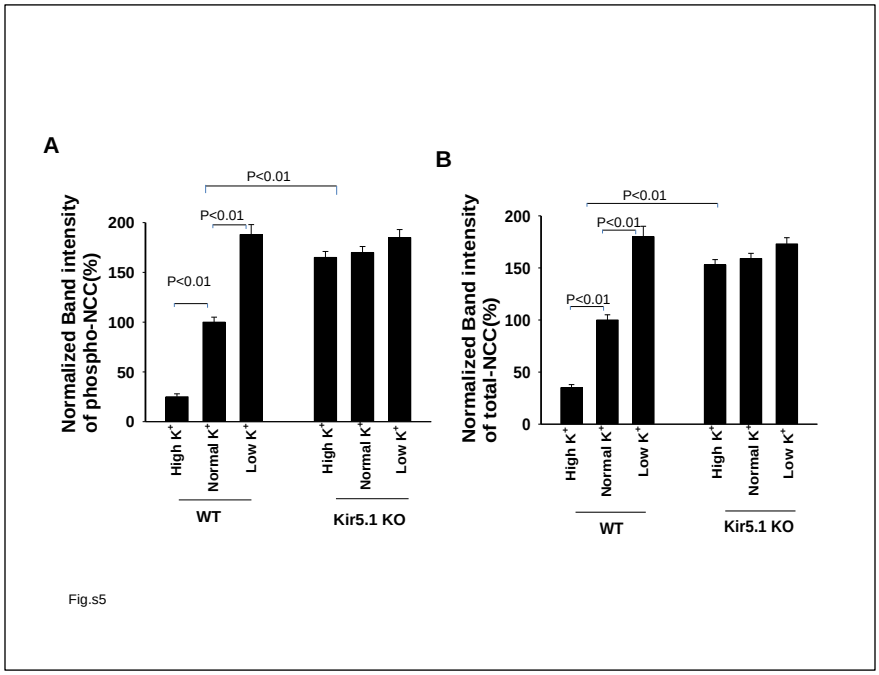

Fig.s5 **Deletion of Kir5.1 abolishes the effect of dietary K^+ intake on tNCC and pNCC**. A bar graph summarizes the normalized band intensity of the above experiments (Figs4) for pNCC (A) and tNCC (B), respectively (n=6 or 7). The significance was determined by one way ANOVA.

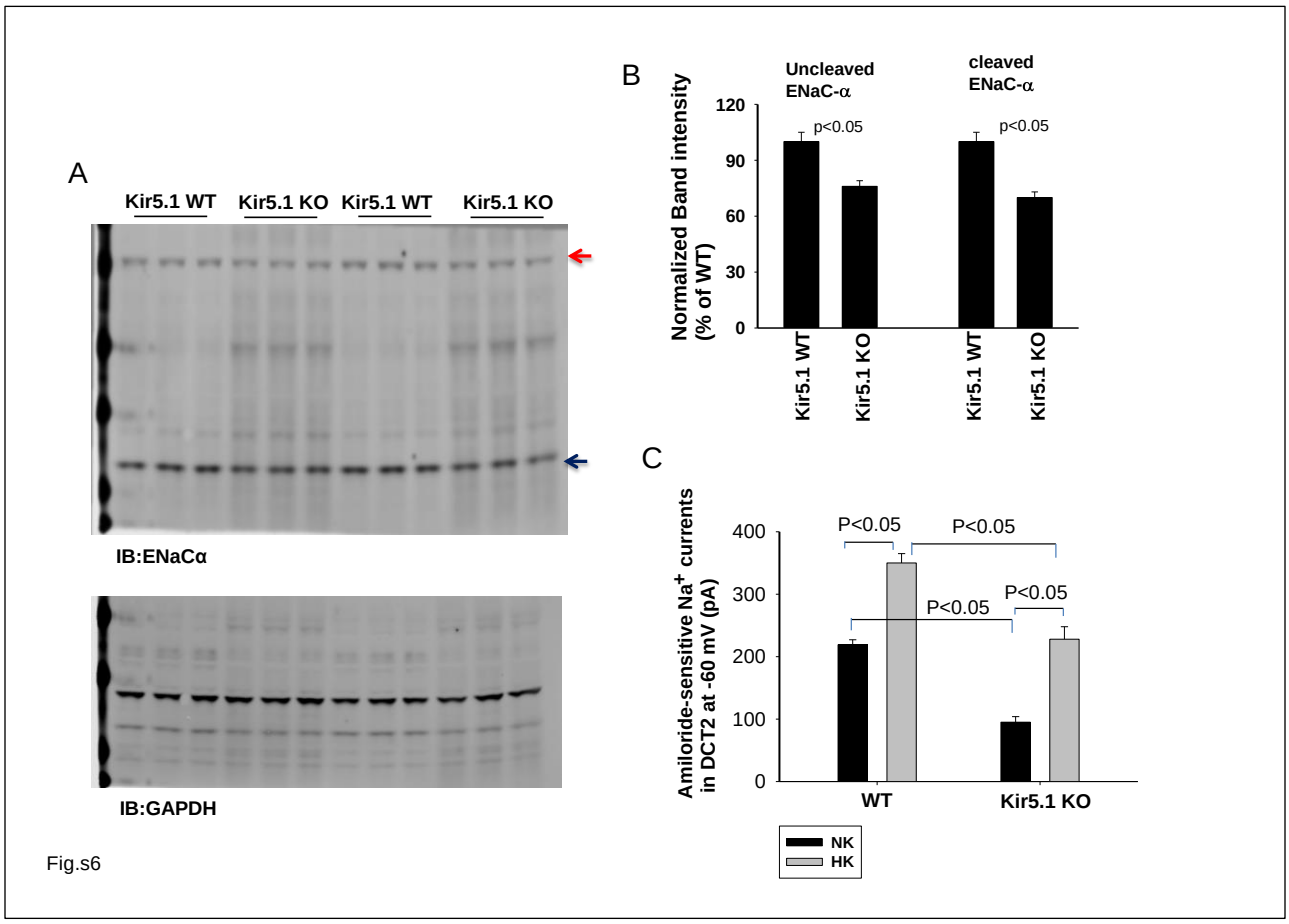

Fig.s6

Fig. s6 **ENaC activity is down-regulated in Kir5.1 KO mice**. (**A**) A immunoblot showing the expression of non-cleaved ENaC-α (red arrow) and cleaved ENaC-α (blue arrow) in Kir5.1 WT and Kir5.1 KO mice on NK. (**B**) A bar graph summarizes the normalized band intensity of the above experiments for non-cleaved ENaC-α and cleaved ENaC-α, respectively (n=6). T test was used for determining the significance. (**C**) A bar graph summarizes the results of experiments in which amiloride (0.1 mM)-sensitive Na^+ currents were measured at -60 mV with perforated whole-cell recording in isolated DCT of WT and Kir5.1 KO mice (n=5 or 6). The significance was determined by one way ANOVA.

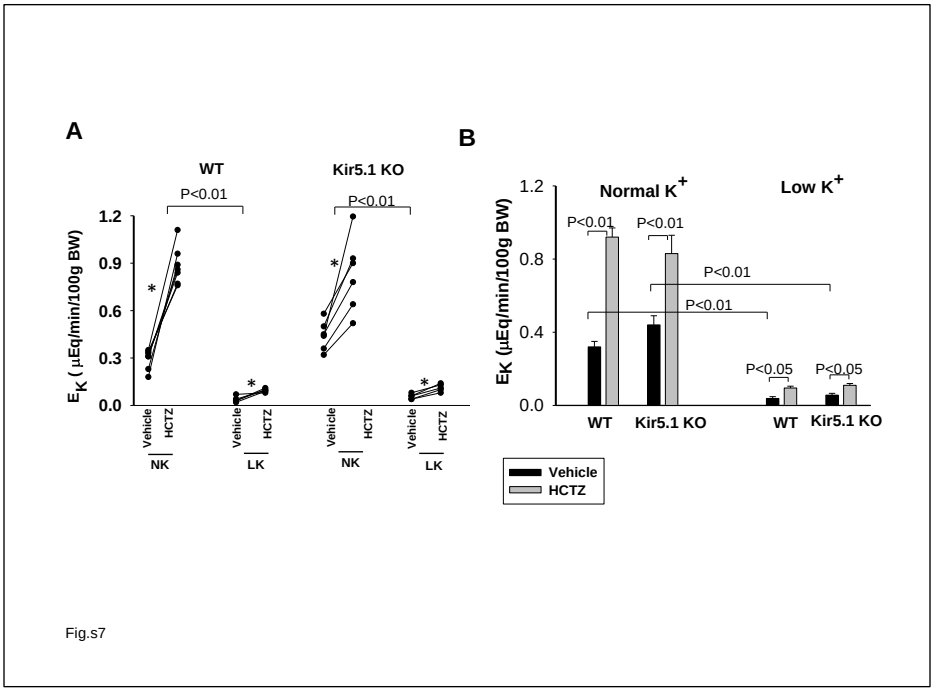

Fig.s7 **K^+ restriction decreases urinary K^+ excretion in Kir5.1 KO mice.** (**A**) A line graph showing the results of each experiment in which the effect of single-dose HCTZ (25 mg/1 kg body weight) on urinary K^+ excretion (E_K) within 120 minutes was measured with the renal clearance method in WT and Kir5.1 KO mice on NK and LK diets for 7 days, respectively. (**B**) A bar graph shows the mean value of E_K and statistical information for all above experiments (n=6). Asterisk indicates a significant difference between vehicle and HCTZ treatment determined by paired student *t* test (P<0.05). The significance between two groups is determined by one way ANOVA.

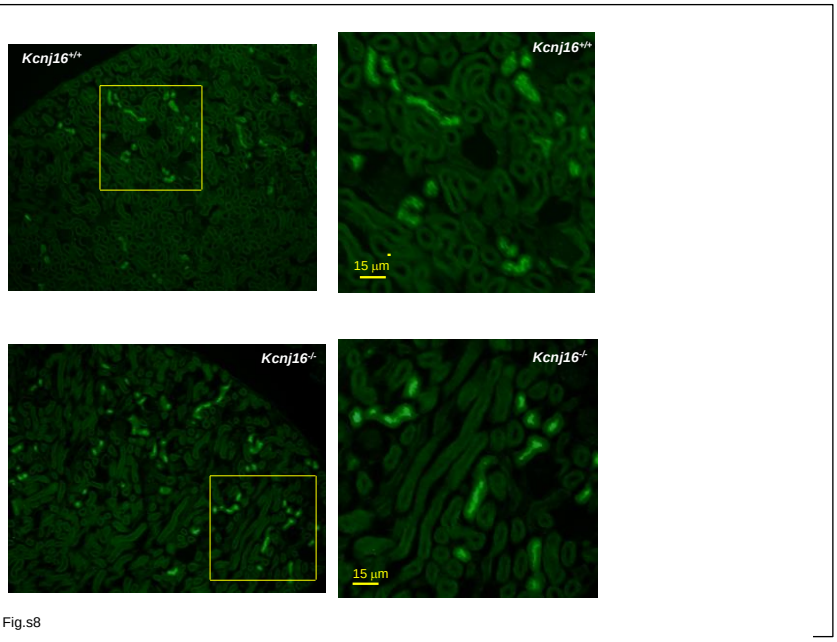

Fig.s8 **Immunostaining of NCC in WT and Kir5.1 KO mice.** An immunostaining shows NCC-positive DCT in WT (top) and in *Kcnj16*$^{-/-}$ mice (bottom). A yellow square of the image is augmented and shown in the corresponding right site.

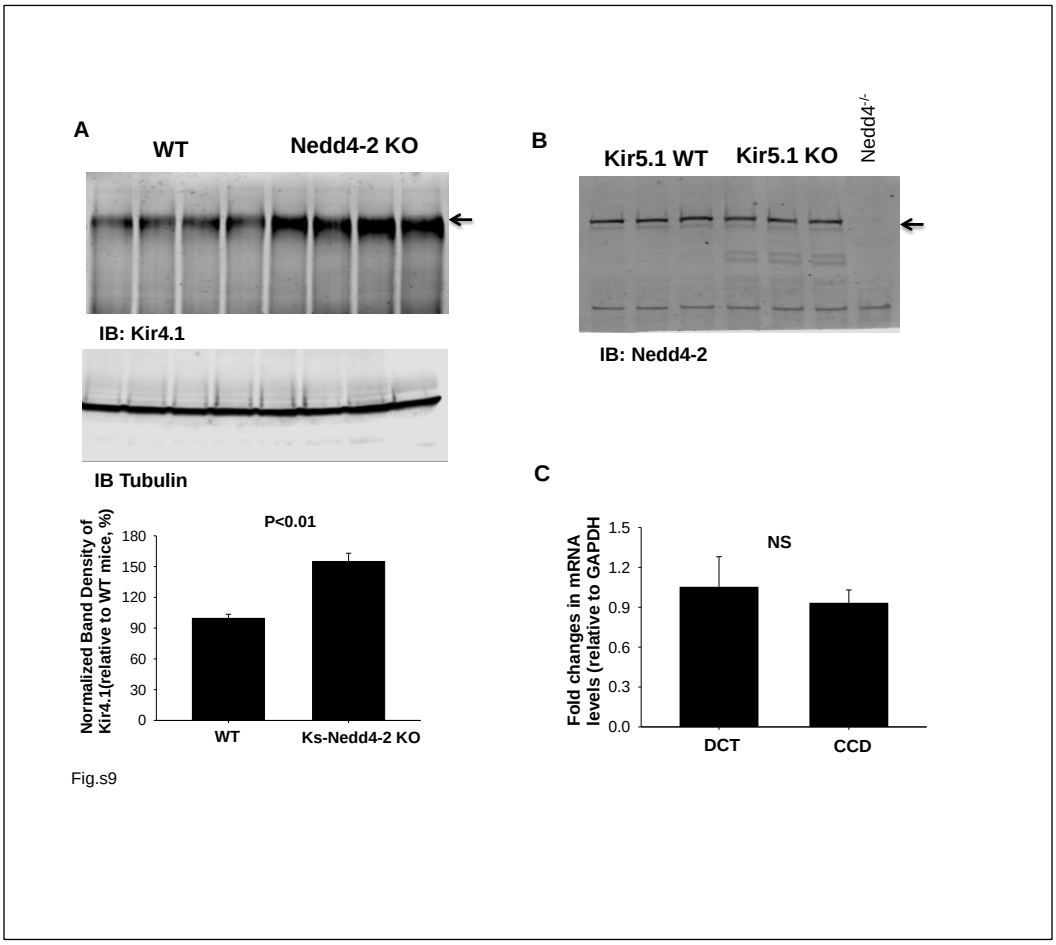

Fig.s9

Fig. s9 **Kir4.1 expression is increased in Ks-Nedd4-2 KO WT mice.** (A) A western blot shows the expression of Kir4.1 (indicated by an arrow) in WT and kidney-specific Nedd4-2 knockout mice (Nedd4-2 KO). The results are summarized in a bar graph showing the normalized band density of Kir4.1 in WT and Ks-Nedd4-2 KO mice (low panel). (B) A western blot shows the expression of Nedd4-2 in WT and Kir5.1 KO mice. The band of Nedd4-2 is indicated by an arrow and the specificity of the antibody is verified with tissue from Ks-Nedd4-2 KO mice. (C) A bar graph shows the relative expression of Nedd4l mRNA in the DCT and CCD of Kir5.1 WT mice.